A data driven approach to update public transport service elasticities

Wong, Howard; Yap, Menno

DOI
10.1016/j.jpubtr.2023.100066

Publication date
2023

Document Version
Final published version

Published in
Journal of Public Transportation

Journal of Public Transportation 25 (2023) 100066

Contents lists available at ScienceDirect

Journal of Public Transportation

journal homepage: www.journals.elsevier.com/journal-of-public-transportation

A data driven approach to update public transport service elasticities

Howard Wong [a,b], Menno Yap [a,c,*]

[a] Transport for London, Public Transport Service Planning, United Kingdom
[b] University College London, Centre for Advanced Spatial Analysis, United Kingdom
[c] Delft University of Technology, Department of Transport and Planning, Delft, the Netherlands

ARTICLE INFO

Keywords:
Elasticity
Generalised journey time
Public transport
Revealed preference
Smartcard data

ABSTRACT

Understanding the passenger demand impacts of public transport service changes is a fundamental aspect of transport planning. The main objective of this study is to derive an updated Generalised Journey Time (GJT) elasticity for urban and metropolitan public transport networks, by applying a revealed preference approach using individual passenger journey data. Based on more than 25 million empirical journeys subject to 9 different service interventions within the Greater London area, we find an average GJT elasticity of −0.61. The value implies that for every 1% increase in generalised journey time, on average public transport demand is expected to reduce by 0.61%, and vice versa. We also find that the demand response to service changes is most elastic during the midday period between the peak hours and most inelastic during the AM peak and early morning, possibly caused by a higher share of mandatory journeys. Our study results confirm the existence of a build-up rate from the initial short-run elasticity to a somewhat stronger longer-run elasticity. Besides, we find that at least within the short- and medium-term demand is more elastic to service degradations compared to service improvements. Our findings imply that it requires more time for demand to increase in response to a service quality improvement, compared to demand to decrease after a service quality reduction.

1. Introduction

1.1. Study relevance

Understanding the passenger demand impacts of public transport (PT) service changes is a fundamental aspect of transport planning. It is important when evaluating the demand changes, revenue impact and wider societal benefits as a result of a change in journey time, service volume or service quality. Such changes include improvements or degradations to the journey quality, planned (track closures, bus network changes) or unplanned (disruptions), in a small or large scale, and can be measured shortly or a long period of time after the service change. For example, a better understanding and forecasting of passenger demand impacts is key during appraisal studies for opening a new PT stop or extending a line to a new development area, as well as when assessing the impact of temporary rail closures due to track maintenance and upgrade works.

A key concept when assessing PT demand changes due to changes in service quality is *service elasticity*. The PT service elasticity represents the demand responsiveness to the change of the public transport service provision. Various types of elasticities exist to estimate the PT demand change resulting from a change of a certain aspect of the PT supply, such as fare elasticities (see Kholodov et al., 2021; Wardman, 2022), in-vehicle time elasticities, service frequency elasticities and journey time elasticities, applied either as short-run or long-run elasticity. A generalised journey time (GJT) elasticity is a comprehensive metric as it captures the demand response resulting from changes to the full passenger journey, including in-vehicle time, out-of-vehicle time and crowding, and the passenger valuation of the respective journey time elements (Balcombe et al., 2004). This GJT elasticity can be applied in scheme appraisals to estimate the PT demand impact of different alternatives, and as such inform the effectiveness of the change planning and investment decision making.

A GJT based service elasticity allows for a more direct and more transparent approach to appraise the benefits (or disbenefits) of schemes. In the absence of a credible GJT elasticity, a more circuitous appraisal method needs to be deployed by monetising the expected journey time savings using a value of time (VOT), which is then converted to financial impacts using a fare elasticity. This method involves various assumptions and often homogenised parameters. Instead, a GJT

* Corresponding author at: Transport for London, Public Transport Service Planning, United Kingdom.
E-mail address: mennoyap@tfl.gov.uk (M. Yap).

https://doi.org/10.1016/j.jpubtr.2023.100066
Received 14 June 2023; Received in revised form 10 August 2023; Accepted 25 September 2023
Available online 28 September 2023

elasticity enables planners to directly estimate the demand impact from the forecast GJT change without further intermediate assumptions, which can directly be converted to revenue impacts based on the average yield per passenger journey (Fig. 1).

1.2. Relevant literature

There is a large body of research on deriving the fare elasticity to understand the PT demand responsive to fare changes. Most of these studies are based on stated preference (SP) experiments or aggregated time-series or cross-sectional analysis. For example, higher fare elasticities are found for longer journeys (Balcombe et al., 2004) and outside the peak hours (Wang et al., 2015). Litman (2019) found that the demand response is larger for fare increases compared to a similar fare reduction. Dargay and Hanly (2002) studied bus fare elasticities in six metropolitan areas in the United Kingdom (excluding London), concluding with an overall short-run fare elasticity of −0.4 and a long-run elasticity of −0.9. Specifically for the London metro and bus network, Jain (2011) found a short-run conditional price elasticity of −0.19 (metro) and −0.35 (bus), respectively. With the availability of large scale, disaggregated passenger data from Automated Fare Collection (AFC) systems, in more recent years some revealed preference (RP) studies have been conducted to derive fare elasticities based on empirical data from smartcards. For example, Wang et al. (2018) evaluated the change from a flat fare to distance based fare system in Beijing, resulting in an average fare elasticity of −0.32. Kholodov et al. (2021) studied the demand response when replacing a fare zone system by a flat fare system in Stockholm, Sweden, finding an overall fare elasticity of −0.46.

The majority of studies to PT journey time elasticities are based on stated preference or aggregated data and focus on mode-specific elasticities with a relatively strong focus on inter-urban rail travel. Wardman (2012) carried out an extensive review and meta-analysis of 427 PT journey time elasticities derived from 69 studies in the UK. This work was further expanded by Wardman (2022), in which a review of journey time elasticities was undertaken based on 741 elasticities drawn from 102 UK studies in total. The journey time elasticities obtained in these studies are primarily derived from stated preference or indirectly from time-series, cross-sectional and pooled aggregated ticket sales data rather than actual journey data. Revealed preference studies directly using disaggregate, individual passenger data are limited. Wardman (2012) found that the mean GJT elasticity among all values for rail travel reviewed was −0.81, and that GJT elasticities did not vary by journey purpose but increase by distance. In Wardman (2022) the mean GJT elasticity found for rail journeys – expressed as a function of journey time (in-vehicle time), service headway and the number of interchanges between stations as time unit equivalent – was −0.90, comparable to the figure found in Wardman (2012). Furthermore, Wardman (2012) found that the long-run GJT elasticity (represented by a one-year period) is around 3.5 times stronger than the short-run elasticity (represented by a four-week period), which has subsequently been revised down to factor 2.3 in Wardman (2022). In the PT industry the Rail Delivery Group (RDG) commissioned research particularly focused on inter-urban train services in the UK and market capture from car and air markets. In the resulting Passenger Demand Forecasting Handbook (PDFH), which serves as reference guide for rail service planning in the UK, the implied GJT elasticity for inter-urban rail journeys is recommended to be between −0.5 and −1.4 (Rail Delivery Group, 2018). In addition, several studies aimed at analysing the PT demand impacts specifically for planned disruptions such as strikes or planned maintenance works. Examples are the evaluation of a 13-day strike in New York City in 1966 (Zhu and Levinson, 2012), PT strikes in California (Ferguson, 1992) and an evaluation of 13 different strikes by Van Exel and Rietveld (2001). Shires et al. (2019) studied the demand impacts of planned engineering works affecting long-distance trains in the UK.

In recent years, PT elasticity research has moved towards using mass-collected smartcard data from AFC systems. Smartcard transaction data collects much more granular details of each passenger journey over a longer period of time. It enables a disaggregated, more extensive demand and origin-destination analysis including the demand response to network changes and the therefrom resulting elasticity. Eltved et al. (2021) used smartcard data to analyse the change in PT demand resulting from a 3-month closure of a rail line in the Greater Copenhagen area. In this study a relatively simple PT rail network is studied without capturing changes in passenger route choice. This method is therefore less suitable for high-density urban PT networks. By analysing PT demand derived from smartcard data before and during four closures, Yap et al. (2018) found that a Generalised Journey Cost elasticity of −0.7 resulted in the highest prediction accuracy to forecast the PT demand reduction during planned closures on the urban tram network of The Hague, the Netherlands. Although based on individual AFC transactions, this study compared aggregated demand by PT line before and during each closure. Yap and Cats (2022) derived a GJT elasticity of −0.99 during a planned track closure on the Amsterdam tram network in 2019 by contrasting GJT and demand changes for affected origin-destination (OD) pairs. This study uses a disaggregated approach to analyse affected origin-destination pairs; however it only considers one planned PT closure in a pre-pandemic context.

1.3. Study contribution

The main objective of this study is to derive an updated GJT elasticity for urban and metropolitan PT networks, by applying a revealed preference approach using individual passenger journey data. A generic method is proposed which can consistently be applied to multiple historic and future case studies, which we apply to several case studies in the Greater London area. Compared to previous studies, the main contributions of this work are the following:

- *Use of extensive, disaggregated data.* Compared to most previous studies which use stated preference data or indirect / aggregated ticket sales data, we derive the PT GJT elasticity based on empirical, individual passenger data from AFC systems. This enables an analysis based on many millions of observed passenger journeys, thus substantially increasing the sample size and representativeness of the source data.
- *Derive mode-agnostic GJT elasticities.* Contrary to most studies which derive elasticities for a specific PT mode (e.g. buses, long-distance

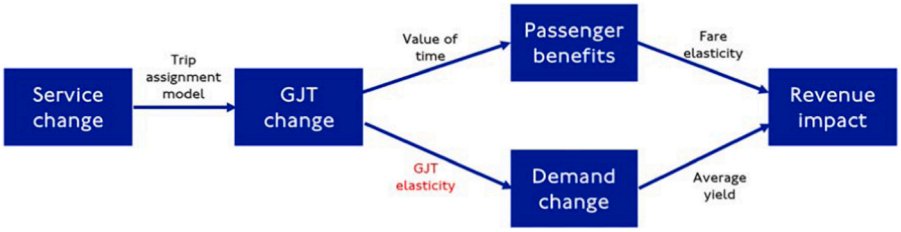

Fig. 1. Appraisal process without (top) and with (bottom) GJT service elasticity.

trains or inter-urban rail), our derived GJT elasticity applies to multimodal PT journeys and are thus mode-agnostic. We link individual passenger journey legs made by different modes together and construct full PT journeys in the urban / metropolitan area of consideration. This is especially relevant given our focus on urban / metropolitan areas, where interchanges between modes are common. Our mode-agnostic approach captures mode changes within the PT system resulting from service changes, which aligns with the pan-PT perspective of public transport authorities in urban / metropolitan areas. It implies that our found elasticities better reflect the full passenger journey and better align with multimodal PT demand matrices used in strategic transport models.

- *Analyse a variety of service improvements and degradations.* Whilst several studies derived service elasticities specifically for closures or disruptions, we study 9 different case studies in London where PT service quality was either improved or (temporarily) reduced. This provides insights in the PT demand response to different types of service changes and helps understanding to what extent the PT demand response is symmetrical for service improvements compared to service degradations. Furthermore, given that many case studies included are post-COVID, our results shine light on the most recent GJT elasticities which reflect recent changes to commuting patterns and PT use in a post-pandemic era.
- *Analyse demand responses over time.* For several case studies we evaluate the demand response at several moments since the intervention (e.g. after 3, 6 and 9 months), providing quantitative evidence on how the GJT elasticity develops over time from short-run to longer-run elasticity.

The key contribution of this study is the development of a generic methodology to derive a PT service elasticity based on a variety of urban / metropolitan PT service changes using millions of individual passenger journeys. Compared to previous studies we use actual, disaggregated passenger journey data and rely on empirical evidence obtained from different types of service changes measured at various time periods since the intervention, providing recent and robust evidence on PT passengers' demand response to service changes.

The paper is structured as follows. In chapter 2 we discuss the methodology used to derive service elasticities and the input data required. Chapter 3 describes the 9 service changes used as case study. Chapter 4 discusses the resulting service elasticity values, including a breakdown of elasticities by time of day, time since intervention and service improvement versus degradation. At last, in chapter 5 we formulate main conclusions and recommendations for follow-up research.

2. Methodology

In this section we first describe the input data processing steps (Section 2.1), followed by the calculation of nominal journey time (NJT) and generalised journey time (GJT) in Section 2.2. In Section 2.3 the calculation of a GJT based service elasticity is defined.

2.1. Data processing

We define the urban or metropolitan PT network of interest as a graph $G(S, E)$ using a L-space network representation. Each node of this graph represents a PT stop $s \in S$ and each edge $e \in E$ reflects a direct PT connection between two stops. The GJT elasticity is calculated from the ratio between the change in volume of PT demand d and the change in GJT between affected origin-destination pairs. This implies that demand data and journey time data is required before and after an intervention or event that prompts a change in the GJT. We use passenger data generated from the AFC system in place for a consistent and controlled comparison of demand levels before and after the intervention. For the specific case of London the AFC data provides a complete coverage of PT journeys made by metro, bus and urban rail within the Greater London area using an Oyster Card or Contactless Payment Card (such as bank cards), thereby enabling a multimodal, mode-agnostic perspective on urban PT demand. Inter-urban and long-distance rail journeys which start or end outside this area are not captured in this data, as they fall outside the study focus on urban PT journeys. Almost all journeys made within the metro network are captured in the AFC data, as 99% of all metro stations in London are equipped with ticket barriers (Transport for London, 2022). For bus journeys AFC data captures the vast majority of passengers, except for a small proportion (ranging between 7% and 12%) of passengers who use magnetic or paper tickets when boarding who are excluded from our analysis.

Each AFC transaction reflects (part of) a passenger journey and contains information on the time and location of both the origin and destination of this journey (leg). For journeys made on the metro and rail network in London, boarding and alighting information is directly empirically available for the entry station and exit station where each passenger is required to tap in and out. For bus journeys where passengers are only required to tap in upon boarding, information on boarding time, boarding stop and route is empirically available. As alighting information is not empirically available, the alighting stop can be inferred using a destination inference algorithm such as proposed by Trépanier et al. (2007), Munizaga and Palma (2012) and Sánchez-Martinez (2017). In this study the destination inference logic as proposed by Gordon (2012) is used, where the downstream alighting stop and alighting time are inferred from Automated Vehicle Location (AVL) data based on the assumption that passengers alight at the stop closest to their subsequent transaction location or closest to their first daily boarding location in case of the last observed PT trip of the day. For each individual AFC transaction this results in empirical boarding information and empirical (for metro and rail) / inferred (for bus) alighting information (Table 1). The destination inference algorithm used to infer the bus alighting stop is widely adopted in science and practice (see the publications by Gordon, 2012; Gordon et al., 2013 and Sánchez-Martinez, 2017) and validated against observed data. The algorithm is able to derive the most plausible alighting stop directly for 75% of the bus journeys (Gordon, 2012). For the remainder of bus journeys – in particular for passengers making one single bus journey which prohibits linking the bus journey to a next journey – the alighting stop is derived probabilistically using the alighting stop distribution for a given boarding stop from the bus journeys for which the alighting stop could be inferred directly.

A PT journey comprises of one or more journey legs made by the same smartcard, traversing on the same or different PT modes. Complete PT journeys are constructed by linking individual AFC transactions made using the same pseudonymised unique card identifier on the same day when several linkage criteria are met. In this work we use the linkage logic as developed by Gordon et al. (2013), meaning that journey legs are linked depending on the interchange time and distance between the alighting stop of the preceding leg and the boarding stop of the succeeding leg to distinguish an interchange movement from a final destination. This step results in the construction of individual, multimodal PT passenger journeys from the first PT origin stop $s_o \in S$ to the ultimate PT destination stop $s_d \in S$.

Table 1
An illustration of the structure of the AFC dataset.

Mode	Route	Start Time	Start Stopcode	End Time	End Stopcode
Metro	-	2022–06–15 08:01:12	778	2022–06–15 08:19:53	729
Bus	43	2022–06–17 16:44:05	BP3065	2022–06–17 16:59:22[a]	BP2336[a]

[a] inferred, not empirically available.

2.2. GJT calculation

For each individual passenger journey i constructed from the AFC data the nominal journey time (NJT) and generalised journey time (GJT) need to be calculated. This means that the observed NJT needs to be converted into GJT by applying various weights to the different components of a journey and its legs. As can be seen in the GJT formulation in Eq. (1), the GJT is the sum of the in-vehicle time t^{ivt}, the out-of-vehicle waiting and walking time t^{wtt} and the number of transfers n^{tf} for each journey. For metro and rail journeys t^{wtt} reflects the initial walking time from the station entry – where the first AFC transaction takes place – to the platform, as well as the platform waiting time. For bus journeys t^{wtt} only captures the initial waiting time at the bus stop. Additionally, t^{wtt} also captures the subsequent interchange walking and waiting time when appropriate. Walking time to the first station or bus stop is not captured within this variable. The coefficients in Eq. (1) reflect the average time valuation of the different journey components. For the case of London $\beta = 2.0$ is used, reflecting that passengers value waiting and walking time on average twice as negative as uncrowded in-vehicle time. This is in line with results from previous Stated Preference and Revealed Preference studies (Wardman, 2004; Bovy and Hoogendoorn, 2005; Yap et al., 2023). A fixed transfer penalty of $\gamma = 3.5$ min is used for each interchange made, consistent with Revealed Preference results found by Yap et al. (2020) and values adopted within UK transport planning practice (Transport for London, 2017). Parameter α reflects the in-vehicle time perception as function of the on-board crowding level. This value typically equals 1.0 as lower bound $\alpha_{\min}$ during uncrowded circumstances when the passenger load q does not exceed the seat capacity c_{seat}, and increases proportional to the on-board standing density (average number of standing passengers per square metre) up to a certain maximum value $\alpha_{\max}$. In line with Transport for London's Business Case Development Manual (Transport for London, 2017) this upper value $\alpha_{\max}$ is set equal to 2.5 when the total (seated plus standing) capacity c_{tot} has been reached. The calculation of α is shown in Eq. (2).

$$GJT_i = \alpha \cdot t_i^{ivt} + \beta \cdot t_i^{wtt} + \gamma \cdot n_i^{tf} \tag{1}$$

$$\alpha = \min\left(\alpha_{\max}, \max\left(\alpha_{\min}, \alpha_{\min} + \frac{(q - c_{seat})}{(c_{tot} - c_{seat})} \cdot (\alpha_{\max} - \alpha_{\min})\right)\right) \tag{2}$$

For bus journeys t^{ivt} can be computed by simply taking the difference between the inferred end time and observed start time of each journey leg in the AFC data, which can be summed over all journey legs constituting a full passenger journey. The initial waiting time at the bus stop t^{wtt} is derived from AVL data containing the actual departure time of each bus from each stop. The actual headway is calculated for each bus route and hour of the day of consideration based on this AVL data. Given the high frequencies of bus routes in urban / metropolitan areas, we can assume that most passengers arrive uniformly distributed at bus stops without explicitly consulting the timetable. This implies that t^{wtt} is equal to half the actual headway for initial boardings. When a passenger interchanges, the interchange walking / waiting time is calculated as the difference between the end time of the previous journey leg and the start time of the consecutive leg. It is not possible to further disentangle interchange waiting time from walking time without making explicit assumptions on the passenger walking speed and without knowledge of the detailed street layout to derive the interchange distance. As the valuation of walking time and waiting time is often found to be similar (see e.g. Wardman, 2004; Yap et al., 2020), this is not expected to impact the accuracy of the GJT calculation. By merging AFC and AVL data the total number of passengers boarding, alighting and on-board a bus is calculated for each individual bus trip and stop. Based on the vehicle capacity of the bus type operating on each route the on-board load q can be contrasted to the capacity, resulting in an average in-vehicle crowding multiplier α for each bus route and hour of each day considered in the dataset. The number of transfers n^{tf} can be computed directly based on the number of journey legs of each journey.

For rail journeys the observed NJT between station entry and station exit includes the in-vehicle time, but also the walking time to/from the platform and waiting time at the platform. For trains not equipped with an Automated Passenger Count (APC) system, train loads and crowding levels are therefore not directly available from the AFC data. The GJT calculation is further complicated as multiple feasible routes can exist between two metro or rail stations in a high-density urban PT network. To address this, we apply an assignment model to derive the route choice probabilities for each feasible route between two stations. Based on these probabilities, the total origin-destination passenger volume is assigned to different routes and aggregated to derive the average train crowding levels for each 15-minute interval. The assignment procedure is calibrated based on loads derived from APC systems for selected lines where available. This process enables the calculation of crowding multiplier α, as well as t^{ivt} based on the observed train running times available from AVL data. The remaining time between station entry and exit is then allocated to t^{wtt}. Similar as for bus journeys it is not possible to separate station walking time from waiting time, as this would require detailed information on the layout and crowding levels of each station to estimate the station walking times. The abovementioned approach computes the GJT between each station pair and provides a regular ratio between the NJT and GJT for each unique station origin-destination pair, day of week and 15-minute time window. Subsequentially, the observed NJT for each individual passenger journey is scaled using the respective ratio to derive the GJT for this journey.

2.3. Service elasticity calculation

In this study we use GJT as passenger focused metric reflecting PT service quality. We identify several PT service changes resulting in either a service improvement or service degradation for affected passengers. To derive the GJT elasticity from AFC and AVL data, we extract PT journeys (Section 2.1) and calculate their generalised journey time (Section 2.2) for selected days before the intervention (ante) and after the intervention (post). Depending on the duration of the service change the post-intervention data is derived for one or multiple time periods since the intervention. As we do not include the exact same passengers in our ante- and post-dataset, we make use of repeated cross-sectional data rather than panel data.

For each individual passenger journey we classify the first origin stop and ultimate destination stop into larger zones. This is of importance to capture passengers who change their first or last PT stop due to this intervention. Furthermore, aggregating to larger zones yields larger absolute demand volumes which is preferable as small absolute values can result in inflated relative demand changes and hence result in unrealistic elasticity values (Eq. (3)). When selecting the appropriate zone size one needs to strike a balance between capturing possible changes in boarding or alighting stop, and limiting the intrazonal flows as this would result in a loss of valuable information. For the spatial aggregation in this study, we classify PT stops into postcode districts due to the relative low proportion of intrazonal journeys and reasonable journey volumes for the origin-destination pairs used in the case studies. In addition, postcode districts are commonly used as part of the addressing and postal system in the UK and cover an area with a recognisable name for the neighbourhood, thus improving interpretability of the results. The Greater London area covering a total surface of 620 km^2 consists of 265 postcode districts, implying an average postcode district size of 2.34 km^2. Temporally weekday demand is aggregated into time periods as this enables us to report elasticity figures broken down by time of day. A timeband is assigned based on the journey departure time: Early (0500–0700), AM Peak (0700–1000), Midday (1000–1600), PM Peak (1600–1900) and Evening (1900–0500). Applying both the spatial and temporal aggregation results in a total PT demand volume $d_{od,t}$ and an average generalised journey time $GJT_{od,t}$ between each origin postcode district $o \in O$ and destination postcode district $d \in D$ in time period

$t \in T$, which can be compared for the ante- and post-intervention dataset.

The calculation of the GJT point elasticity $\eta_{od,t}^{GJT}$ for each origin-destination-timeband combination is shown in Eq. (3). When using repeated cross-sectional data, it is important to correct for background demand changes unrelated to the intervention itself. Background demand changes between the baseline period prior to intervention and monitoring period after intervention can stem from macro-level changes such as seasonality, school holidays, COVID-19 travel restrictions or generic post-pandemic PT demand recovery. It is often challenging to separate the demand changes resulting from the intervention from other drivers impacting demand, particularly in an era still affected by the pandemic where PT demand has shown to be much more volatile than pre-pandemic. In our work we have introduced an additional global demand adjustment factor d^c to scale $d_{od,t}^{ante}$ (Eq. (3)). We derive the total number of PT journeys made on the entire PT network of consideration from the AFC data and determine a background demand growth factor d^c between baseline and monitoring period. We correct $d_{od,t}^{ante}$ by d^c, meaning that for the OD pairs included it is implicitly assumed that all demand changes other than the background correction are attributed to the intervention. Whilst this approach has its limitations, it is not trivial how to use a more disaggregated background correction factor (e.g. specifically for selected bus routes, rail lines or London areas), since we consider multimodal PT journeys which can traverse several parts of the city using various modes and lines. We therefore opt for a relatively simple, generic correction term. We have performed a sensitivity analysis to test the extent to which the found elasticity changes when a lower or higher generic demand correction factor d^c is applied. This sensitivity analysis resulted in relatively limited changes of the value of η^{GJT}, confirming that our results are robust against variations in d^c.

$$\eta_{od,t}^{GJT} = \frac{\left(\frac{d_{od,t}^{post}}{d_{od,t}^{ante} \bullet d^c}\right) - 1}{\left(\frac{GJT_{od,t}^{post}}{GJT_{od,t}^{ante}}\right) - 1} \tag{3}$$

The total GJT elasticity η^{GJT} for a case study is calculated by taking the demand-weighted average GJT elasticity over all included origin-destination-timeband combinations (Eq. (4)). We combine a top-down and bottom-up approach to determine which PT journeys to include in the elasticity calculation for a given intervention. Based on the geographical location of the intervention we loosely define a list of postcode districts around this intervention for which PT journey times are likely affected. We first filter top-down for journeys that either start or finish in one of the listed postcode districts. As not necessarily all journeys to or from postcode districts near the intervention will be affected, secondly we filter bottom-up and only include origin-destination-timeband combinations satisfying the following four conditions.

- First, we set a minimum GJT change threshold δ (either as increase or decrease) resulting from service changes, to only include OD pairs where the GJT notably changed after the intervention. In this study we set $\delta = 4\%$: based on the average GJT of 38.8 min for our case study network, this corresponds on average to a minimum GJT change of 1.5 min and a minimum unweighted journey time change of just over 1 min. Depending on the average journey time of the study area of consideration, this threshold can be adjusted accordingly.
- Second, there should not be more than 10% demand increase (for service degradations) / decrease (for service improvements). Generally a demand increase is expected for service improvements, meaning that an observed demand reduction is not expected to be related to the service change. However, to account for the possibility that certain OD pairs might be negatively affected despite an overall positive service change, we accept the inclusion of OD pairs with a limited observed demand reduction during a service improvement (and vice versa for service degradations).
- Third, we set $\left|\eta_{od,t}^{GJT}\right| \leq \varepsilon$, with $\varepsilon = 3$ in this study. The calculation of a point elasticity is naturally sensitive to small absolute demand volumes and small GJT changes. In case $d_{od,t}^{ante}$ is small it is possible that the numerator of Eq. (3) becomes very large, resulting in an inflated elasticity value especially in case the GJT change in the denominator is small. Based on the range of GJT elasticity values found in previous studies we exclude OD pairs where the elasticity value is unrealistically large in absolute terms as a result of this effect.
- Fourth, we exclude intrazonal journeys where origin and destination postcode districts are equal.

$$\eta^{GJT} = \sum_{t\in T}\sum_{o\in O}\sum_{d\in D}\eta_{od,t}^{GJT} \bullet d_{od,t}^{ante} \Big/ \sum_{t\in T}\sum_{o\in O}\sum_{d\in D} d_{od,t}^{ante} \tag{4}$$

Furthermore, we also estimate several pooled models where we combine the observations from multiple case studies in order to derive an overall GJT elasticity across all case studies and segmented for different times of day and different types of interventions. Where the elasticity defined in Eq. (3) implies a linear relation between a relative change in GJT and a relative demand change, additionally we assess whether using a non-linear function provides a better fit. In addition to a simple linear function, we therefore estimate non-linear functions by fitting the datapoints of our total pooled model to a power function, logarithmic function and a negative exponential function. The latter is a commonly used impedance function in transport economics (Eq. (5)) (see for example Neutens et al., 2010). In this equation $\%\Delta GJT$ reflects the relative change in GJT – equivalent to the denominator of Eq. (3) – whilst $\%\Delta d$ reflects the relative change in PT demand – equivalent to the numerator of Eq. (3). Parameters κ, λ and μ represent the scale parameter, the growth / decay rate parameter of the exponential function and a constant, respectively. For this function we set parameter μ equal to $-\kappa$ to fit the curve through the origin, so that no demand change is predicted if there is no GJT change.

$$\%\Delta d = \kappa \cdot \exp(-\lambda \bullet \%\Delta GJT) + \mu \tag{5}$$

3. Application

3.1. London case study area

We demonstrate the proposed methodology on 9 separate case studies whereby there were various significant changes to the PT network between 2018 and 2022 in the Greater London area. These cases cover positive and negative changes to the service provision, have long and short-term impact, have localised and city-wide implications and affect bus, metro and urban rail in various extents. Depending on the duration of the service change and current data availability we extract the demand and GJT changes within the first 3 months after intervention, between 3 and 6 months, 6–9 months and 9–12 months. This provides a range of service elasticities from short-run when measured within the first three months since the intervention towards a longer-run elasticity. In total, 16 case-timepoint combinations are included in our study. Across all 9 case studies, 25.48 million passenger journeys (before each intervention) are included in our analysis, meaning that our estimation results are based on a large body of empirical evidence. These cases are described in more detail in Section 3.2.

The passenger demand and journey time data in our study is derived from the AFC and AVL system of Transport for London as transport authority of the Greater London area. Transport for London maintains an AFC system that accepts Oyster Card and Contactless Payment Cards (CPC) across its bus and rail networks. Rail network AFC data includes all travel data from the London Underground metro network (consisting of 11 metro lines) and from all urban rail networks including London Overground, the newly opened Elizabeth Line and journeys made on

National Rail trains within the Greater London boundary using Oyster or CPC. The AFC system is supplemented by a destination and transfer inference system – known as ODX – that connects legs to journeys and infers missing leg destination information using card-level journey pattern data and service performance data, performing the data processing steps described in Section 2.1.

3.2. Case study description

Table 2 summarises the main characteristics of each case study, including the date of the service change and the selected period for the pre-intervention baseline and post-intervention monitoring period. In both the ante- and post-dataset we only focus on travel behaviour in the mid-week (Tuesday, Wednesday, Thursday) when the demand pattern and reason for travel is most stable and predictable.

Case 0_HSB refers to the closure of Hammersmith Bridge for vehicular traffic due to engineering issues since April 2019. The closure severed a number of bus routes used to operate across River Thames linking Hammersmith town centre and the suburbs of Barnes and Mortlake in southwest London. In case 1_GOB, the service on the orbital Gospel Oak-Barking (GOB) rail line operated by London Overground was suspended for four weeks when a freight train derailed in January 2020 and damaged a large section of tracks. The Northern line Extension (case 2_NLE) opened in September 2021, connecting the Nine Elms Battersea opportunity area with many housing and office developments to the London Underground metro network. Four different monitoring periods are included since the opening of this two-stop extension. The last monitoring period in September 2022 also captures the doubling of the service frequency on this extension since June 2022.

The Northern Line Closure (case 3_NLC) was a major closure of the Bank branch on the London Underground Northern line for 17 weeks from January 2022. The closure severed a direct access from south London to the City where the main financial district is located. As forecast traffic impact was significant, Transport for London carried out a big communication campaign to inform prospective passengers and businesses well ahead of the closure, and laid out additional bus services on routes that were expected to be exceptionally busy. The closure happened when the Covid Omicron variant was highly prevalent in the UK, meaning that background demand was heavily suppressed. In Fig. 2 the top-down spatial filtering process of journeys as addressed in Section 2.3 is illustrated for this case study. It shows the selected postcode districts in the vicinity of the service change, meaning that only passenger journeys to or from the identified postcode districts are included in the dataset for this specific case study.

Case 4 focuses on the demand response related to the opening of the new Elizabeth Line. In May 2022 the central section was opened. This entirely new rail line provides direct, fast connections between central London and southeast London (Canary Wharf financial area) and alleviates crowding on busy metro lines. In November 2022 two train lines – a western line from Reading previously terminating at Paddington and an eastern line from Shenfield previously terminating at Liverpool Street station – were integrated into the Elizabeth Line. Both the western section (Case 4w_EZL) and eastern section (Case 4e_EZL) were connected under central London through the new central section which was opened in May 2022. As one of the largest transport projects in Europe, the opening and through-running of Elizabeth Line services has resulted in major journey time reductions. For Case 4_EZL we only include monitoring points after completion of the full service pattern including the through-running of the western and eastern section, to capture a more stable demand pattern.

Fig. 2. Selection of relevant postcode districts for Northern Line Closure case study.

Case 7_MHE reflects a small timetable change on the Northern Line metro where the shuttle operation on the relatively quiet branch between Mill Hill East and Finchley Central was replaced by a direct connection to central London. This improvement only applied to the midday period between the peak hours. Lastly, case 8_BRE is the 4.5 km extension of the London Overground rail service from Barking to the new housing development area Barking Riverside in northeast London. As this area was previously only connected by bus, the provided train services result in substantial, albeit localised, journey time reductions.

Table 2
Case study characterisation.

Case	Description	Service Impact	Duration	Mode Affected	Intervention Date	Baseline Period	Monitor Period
0_HSB	Hammersmith Bridge Closure	Negative	> 12 months	Bus	April 2019	Sep-Nov 2018	3m: July 2019 6m: Sep-Nov 2019
1_GOB	Freight train derailment Gospel Oak – Barking	Negative	< 1 month	Rail	January 2020	Nov 2019	1m: Jan-Feb 2020
2_NLE	Northern Line Extension (Battersea)	Positive	structural	Metro	September 2021	Aug-Sep 2021	1m: Oct 2021 3m: Dec 2021 6m: March 2022 12m: Sep 2022
3_NLC	Northern Line Closure (Bank)	Negative	4 months	Metro	January 2022	Nov 2021	1m: Jan 2022
4_EZL	Opening Elizabeth Line (central section)	Positive	structural	Rail	May 2022	May 2022	6m: Nov 2022 9m: Jan 2023
4e_EZL	Opening Elizabeth Line (eastern section)	Positive	structural	Rail	November 2022	May 2022	3m: Jan 2023
4w_EZL	Opening Elizabeth Line (western section)	Positive	structural	Rail	November 2022	May 2022	3m: Jan 2023
7_MHE	Northern Line timetable change (Mill Hill East)	Positive	structural	Metro	September 2021	Aug-Sep 2021	3m: Dec 2021 6m: March 2022
8_BRE	LO rail extension Barking Riverside	Positive	structural	Rail	July 2022	June 2022	3m: Sep 2022 6m: Jan 2023

4. Results and discussion

4.1. Results

The estimated GJT elasticities η_t^{GJT} for each case study and monitoring period are summarised in Table 3, with the t-statistic indicated between parentheses. The negative values of the GJT elasticity for all cases and all times of the day demonstrate a plausible, negative relation between journey time change and demand change. For all service degradations (0_HSB, 1_GOB, 3_NLC: see Table 3) this implies that the journey time increase following from the removal and detouring of direct services results in an overall PT demand reduction. Conversely, the service extensions, frequency increases and introduction of through-running trains in all service improvement cases result in an overall demand increase and subsequentially a revenue increase. As mentioned in Section 3.2, the service improvement in Case 7_MHE only applies to the midday period between the AM and PM peak. Therefore, no elasticity values are provided for the other time periods. The Barking Riverside Extension case (8_BRE) is the only case returning a statistically insignificant elasticity value for Early ($t \leq |1.96|$, $p \geq 0.05$). All other cases and time periods show significant results ($p < 0.05$). With the exception of the Midday elasticity for the Mill Hill East Case (7_MHE_6), the absolute t-value is larger than 2.58 for all other cases and time periods, confirming that those results are highly statistically significant ($p < 0.01$).

The empirical results from all case studies together are shown in a scatterplot in Fig. 3. Each point reflects the relative change in GJT and PT demand for an origin-destination-timeband combination included in the elasticity calculation. The size of the dots reflects the absolute pre-intervention demand volume. As mentioned in Section 2.3, we experimented fitting a simple linear function, an exponential function, a logarithmic and a power function to obtain a best fitting curve. From these models fitting an exponential function yielded the highest r^2 score. In Fig. 3 the best fitting exponential function is shown for the pooled model with all cases and time periods together. The results from Table 3 show there is quite some variance in found elasticity values between different case studies, which explains why the prediction accuracy when fitting one generic function for all cases together (r^2 =0.52) is not very high. A higher r^2 is obtained when fitting a curve for each individual case study. With parameter value λ= 0.73 using Eq. (5), we find that in line with transport economics theory a negative exponential function results in the highest fit overall. As mentioned in Section 2.3, parameter μ (−1.20) is constrained to be equal to $-\kappa$ (1.20) to fit the curve through the origin. The r^2 for the exponential curve (0.52) is somewhat higher than the r^2 when fitting a simple linear function through the data points of the pooled model (r^2 =0.45). This indicates that applying a linear elasticity figure can be a reasonable approximation for the expected PT demand response to service changes, albeit that a more accurate forecast can be obtained when applying the fitted negative exponential function.

4.2. Discussion and policy implications

4.2.1. Results by time period

The overall GJT elasticity found from the pooled model across all cases and time periods is −0.61 and highly statistically significant (bottom right cell in Table 3). This value implies that a 1% increase in GJT on average results in a 0.61% reduction in PT demand, and vice versa. When comparing this overall value to previously found figures in literature, we conclude that this value falls within a plausible range. The value is somewhat less negative than the average value of −0.81 and −0.90 found by Wardman (2012) and Wardman (2022). However, figures from the latter are predominantly based on inter-urban and long-distance rail journeys where average journey lengths are substantially higher than within an urban or metropolitan PT network. When studying fare elasticities (Balcombe et al., 2004) and journey time elasticities (Wardman, 2012), both studies conclude that elasticities become more negative with increasing journey length. It is therefore expected to find a somewhat less negative GJT elasticity in our study entirely based on urban / metropolitan case studies. Furthermore, our overall GJT value is within the plausible GJT range [−0.5,−1.4] as recommended by the Rail Delivery Group (2018).

Based on the pooled model results shown in the last row of Table 3 we are able to compare the GJT elasticity between different times of the day. It should be noted that we currently only included weekday data in our study, meaning that the time breakdown as presented does not necessarily apply to weekend days. We find that the PT demand response is strongest during the midday period (−0.68), followed by the PM peak (−0.64), AM peak (−0.55), evening (−0.53) and early morning (−0.46). This can be explained by the different mix of journey purposes for which passengers use the PT network during different times of the day. The proportion of journeys with a discretionary character such as leisure or shopping is highest during midday, followed by the PM peak with typically a mix between commuting and leisure / shopping journeys. The less mandatory character of these trips means that a stronger demand response to service improvements or reductions is expected, as there is a higher degree of flexibility for these passengers to change mode, destination or date of travel. This finding is consistent with the conclusion by Wang et al. (2015) on fare elasticities, where a more

Table 3
GJT elasticity estimation results.

Case	η^{GJT}_{Early}	η^{GJT}_{AM}	η^{GJT}_{Midday}	η^{GJT}_{PM}	$\eta^{GJT}_{Evening}$	η^{GJT}
0_HSB_3	-0.47 (−4.13)	-0.71 (−3.86)	-0.66 (−16.3)	-0.66 (−11.8)	-0.73 (−6.49)	**-0.67 (−17.0)**
0_HSB_6	-1.10 (−8.38)	-0.90 (−33.8)	-0.69 (−39.8)	-0.76 (−40.9)	-0.80 (−30.6)	**-0.78 (−68.8)**
1_GOB_1	-0.45 (−20.4)	-0.30 (−44.7)	-0.31 (−41.9)	-0.33 (−43.9)	-0.18 (−29.5)	**-0.30 (−81.4)**
2_NLE_1	-0.46 (−13.2)	-0.52 (−24.8)	-0.22 (−13.0)	-0.60 (−20.6)	-0.46 (−14.6)	**-0.43 (−36.0)**
2_NLE_3	-0.18 (−12.1)	-0.47 (−23.2)	-0.59 (−25.4)	-0.38 (−19.0)	-0.38 (−20.3)	**-0.47 (−45.8)**
2_NLE_6	-0.24 (−12.8)	-0.69 (−29.2)	-0.41 (−18.6)	-0.61 (−27.3)	-0.37 (−24.2)	**-0.48 (−47.2)**
2_NLE_12	-0.51 (−16.4)	-0.16 (−16.3)	-0.65 (−29.9)	-0.71 (−23.0)	-0.36 (−23.2)	**-0.56 (−50.9)**
3_NLC_1	-0.60 (−32.5)	-0.79 (−57.0)	-0.68 (−55.1)	-0.77 (−60.7)	-1.01 (−54.9)	**-0.79 (−121.7)**
4_EZL_6	-0.59 (−17.2)	-0.29 (−25.0)	-1.01 (−43.3)	-0.56 (−30.1)	-0.50 (−33.6)	**-0.64 (−70.7)**
4_EZL_9	-0.54 (−20.3)	-0.58 (−25.1)	-1.11 (−45.5)	-0.75 (−34.0)	-0.40 (−30.9)	**-0.73 (−74.3)**
4e_EZL_3	-0.72 (−14.5)	-0.75 (−16.3)	-1.04 (−21.8)	-0.74 (−16.0)	-1.15 (−25.1)	**-0.90 (−41.4)**
4w_EZL_3	-0.80 (−11.5)	-0.77 (−12.4)	-0.93 (−18.0)	-0.82 (−17.7)	-1.34 (−18.6)	**-0.92 (−34.3)**
7_MHE_3	n/a	n/a	-0.54 (−3.70)	n/a	n/a	**-0.54 (−3.70)**
7_MHE_6	n/a	n/a	-0.57 (−2.43)	n/a	n/a	**-0.57 (−2.43)**
8_BRE_3	n/s (−1.43)	-0.40 (−7.78)	-1.18 (−13.9)	-0.84 (−6.98)	-0.11 (−6.00)	**-0.63 (−18.1)**
8_BRE_6	n/s (−1.77)	-0.64 (−8.36)	-1.19 (−12.2)	-0.83 (−7.62)	-0.52 (−4.95)	**-0.78 (−17.3)**
Pooled (all)	*-0.46 (−54.7)*	*-0.55 (−106.6)*	*-0.68 (−114.9)*	*-0.64 (−112.7)*	*-0.53 (−103.8)*	*-0.61 (−228.2)*

t-values in parentheses.
n/s: elasticity not statistically significant ($t \leq |1.96|$).

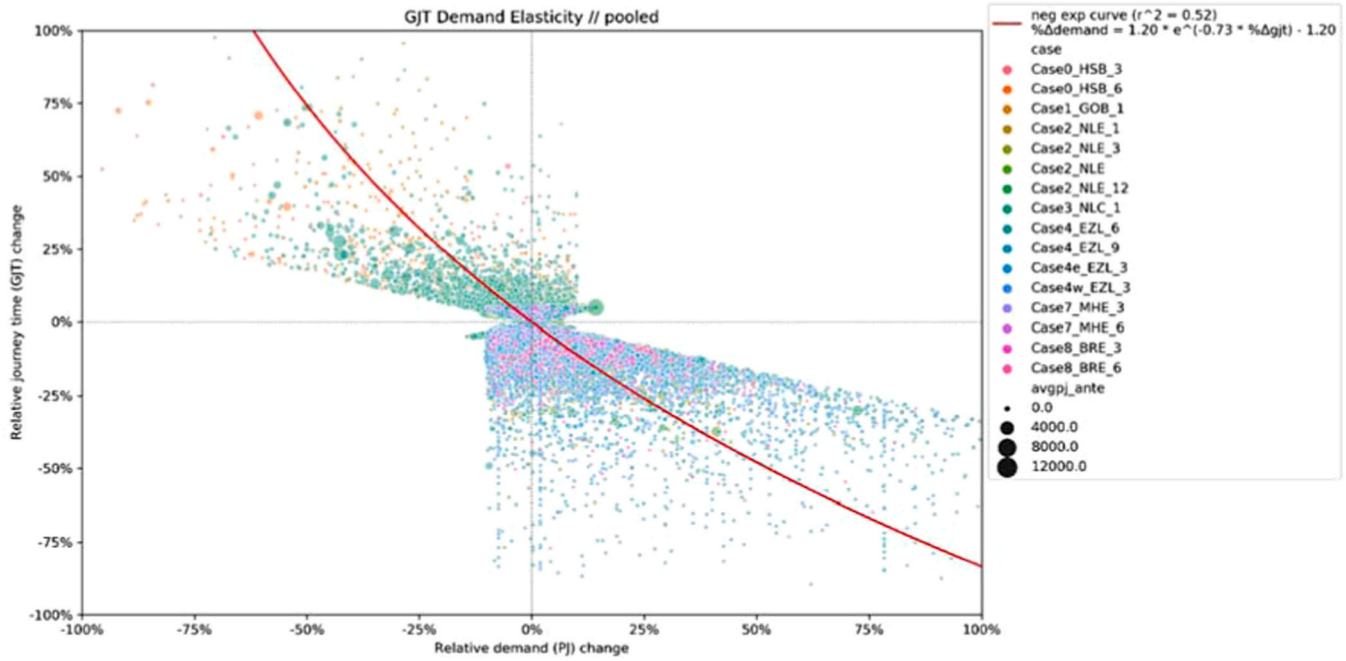

Fig. 3. Scatterplot with observed changes in GJT and demand.

negative value was found outside the peak hours. Journeys made during the AM peak and early morning are typically composed of a high proportion of commuting trips with a more mandatory character, which explains the weaker demand response found for these two periods.

We might hypothesise that the difference in found elasticity between the AM peak (−0.55) and early morning (−0.46) is related to the share of blue-collar workers, especially in a post-pandemic context. Since the COVID-19 outbreak there is a higher degree of flexibility for some white-collar (office) workers to work from home, whilst this is not an option for jobs where physical attendance is required, such as construction or medical workers. Specifically within the context of London blue-collar workers tend to travel earlier in the morning (for example to start shift work) compared to office workers, which is a possible explanation for the less elastic demand observed during the early morning period. The relatively weak demand response found in the evening might be driven by the fact that most of these journeys are return journeys to home, for which the decision to travel was taken earlier in the day. Another explanation is that the average value-of-time in the evening is relatively low due to the low share of commuting and business trips, meaning that passengers are less sensitive to journey time changes compared to other times of day.

4.2.2. Results by case study

Table 4 presents the elasticities per case study and time since intervention. For all case studies with more than one monitoring point we can see that the elasticity gradually becomes more negative when more time has passed since the intervention, confirming a build-up rate before the PT demand response to a journey time change stabilises.

The relatively low elasticity of −0.30 for the 1_GOB derailment case study can be explained by the unplanned nature of the disruption – an unplanned train derailment – combined with a relatively short duration of the total disruption. It is possible that passengers had fewer opportunities to adjust their travel plans unexpectedly on short notice, or that they were willing to accept a longer journey time due to the clearly temporary nature of this event. In contrast, we find a strong elasticity of −0.79 for the 3_NLC Northern Line closure compared to other service reductions within the first three months since the intervention. This might be explained by the extensive travel demand management campaign which was rolled out before and during this closure. As overcrowding on alternative routes was expected, Transport for London carried out a big information campaign on alternative routes and travel times, working together with large companies affected by this closure, whilst supplying additional bus capacity around the impacted area. It is plausible that this has resulted in more awareness and a stronger demand response from affected passengers.

Furthermore, for all three Elizabeth Line cases we observe a relatively strong demand response. This is possibly not only driven by the pure changes in journey time, but also by the substantial improvement in travel comfort and ambiance. In contrast to parallel metro routes, Elizabeth Line trains are equipped with air conditioning, are more spacious and operate from brand new stations, which might have contributed to a larger behavioural change. We can also conclude that the elasticity for Case 4_EZL – serving an entirely new route – is somewhat lower than the elasticities for Case 4e_EZL and 4w_EZL – where an existing train line is integrated into the Elizabeth Line network. One

Table 4
Elasticities per case study and time since intervention.

Case	Description	0–3 months	3–6 months	6–9 months	9–12 months
0_HSB	Hammersmith Bridge Closure	-0.67	-0.78		
1_GOB	Freight train derailment Gospel Oak – Barking	-0.30			
2_NLE	Northern Line Extension (Battersea)	-0.43	-0.47	-0.48	-0.56
3_NLC	Northern Line Closure (Bank)	-0.79			
4_EZL	Opening Elizabeth Line (central section)		-0.64	-0.73	
4e_EZL	Opening Elizabeth Line (eastern section)	-0.90			
4w_EZL	Opening Elizabeth Line (western section)	-0.92			
7_MHE	Northern Line timetable change (Mill Hill East)	-0.54	-0.57		
8_BRE	LO rail extension Barking Riverside	-0.63	-0.78		

hypothesis is that this difference relates to the bigger leap made in terms of connectivity for Case 4_EZL, which means that the existing market will be relatively smaller because travel was previously difficult. The demand build-up is likely to take longer because a larger shift in embedded travel patterns is needed as more people need to move home or job to take advantage of the newly served area. In Fig. 4 the spatial distribution of GJT impacts is illustrated for Case 4e_EZL (left) for all journeys starting at one specific postcode district (Ilford: IG1) and for Case 4w_EZL(right) for all journeys starting in postcode district UB2 (Southall).

4.2.3. Segmented results

The different case studies are grouped into segments to estimate several segmented pooled models. Table 5 shows that when grouping only data points from the last monitoring period available for each case study – reflecting a more steady state situation – the average elasticity increases to −0.68. Similarly, we find that the overall elasticity 6+ months after the intervention (−0.63) is ~10% higher than the elasticity resulting from cases monitored within the first six months (−0.58). When comparing the 12-month elasticity found for case 2_NLE to the elasticity within first month (Table 4), the elasticity increased by 30%. Both outputs confirm the existence of a build-up rate from the initial short-run elasticity to a somewhat stronger longer-run elasticity.

Furthermore, we find a stronger demand response in the event of a service reduction (−0.68) compared to a service improvement (−0.59). This implies that it requires more time for demand to increase in response to a service quality improvement, compared to demand to decrease during a service quality reduction. The latter is consistent with the finding from Litman (2019) on fare elasticities, where a stronger demand response is found for fare increases compared to a similar fare reduction. The difference can be explained by the fact that a service reduction directly impacts the current PT passengers affected by this, prompting a demand response. Conversely, for service improvements it takes time for the existing resident and employment population to adjust their travel pattern to take advantage of the intervention and optimise the GJT of their journeys, and for new population to be attracted to an area due to its improved connectivity. These findings show that at least in the short- and medium-run, demand is more elastic to service degradations than service enhancements. The post-intervention measurement points in our case studies do no span over more than 12 months since the service change. Therefore, this study does not provide sufficient evidence to conclude whether this asymmetric demand response continues to proliferate even in the long-run (i.e. 1–3 years after intervention) or whether the service improvement elasticity eventually will catch up with the service degradation elasticity over time.

When segmenting the case studies into large scale interventions (2_NLE, 3_NLC, 4_EZL, 4e_EZL, 4w_EZL) and smaller scale interventions (0_HSB, 1_GOB, 7_MHE, 8_BRE), we find a more elastic demand response (−0.62) for large scale interventions compared to smaller scale interventions (−0.50). It suggests that the marginal demand response to GJT changes increases when the absolute GJT change is larger. This finding aligns with the more elastic demand response found for the Elizabeth Line case studies – each of them resulting in relatively large and wide-spread journey time reductions – and illustrates that there is some degree of non-linearity in the relation between GJT and demand as shown in Fig. 3.

Table 5
Elasticities for segmented pooled models.

Pooled Model Segment	GJT elasticity
All cases and time periods	-0.61
Last monitoring point per case	-0.68
Time since intervention < 6 months	-0.58
Time since intervention 6+ months	-0.63
Service improvement	-0.59
Service reduction	-0.68
Large scale intervention	-0.62
Smaller scale intervention	-0.50

4.2.4. Implied fare elasticity

For further validation we can use the overall service elasticity of −0.61 as found in our study to calculate the implied fare elasticity based on the relation between η^{GJT}, η^{fare}, GJT, the average Value-of-Time (VOT) and yield per journey (*fare*) as shown in Eq. (6).

$$\eta^{GJT} = \eta^{fare} \bullet VOT \bullet \left(\frac{GJT}{fare}\right) \quad (6)$$

Table 6 shows the values specifically for the London transport network as derived for June 2022 as indicative values, from which the implied fare elasticity $\eta^{fare} = -0.18$ is calculated. This value is very similar to the value found for the short-run metro fare elasticity in London by Jain (2011) (−0.19) which is also used for business case

Table 6
Calculation of implied fare elasticity.

Variable	Value
η^{GJT} (GJT elasticity)	**-0.61**
VOT (Value-of-Time: all modes) (£/minute)	£0.17
GJT (network average GJT: all modes) (minute)	30.24
Fare (average fare per paid journey: all modes) (£)	£1.55
η^{fare} (implied fare elasticity)	**0.18**

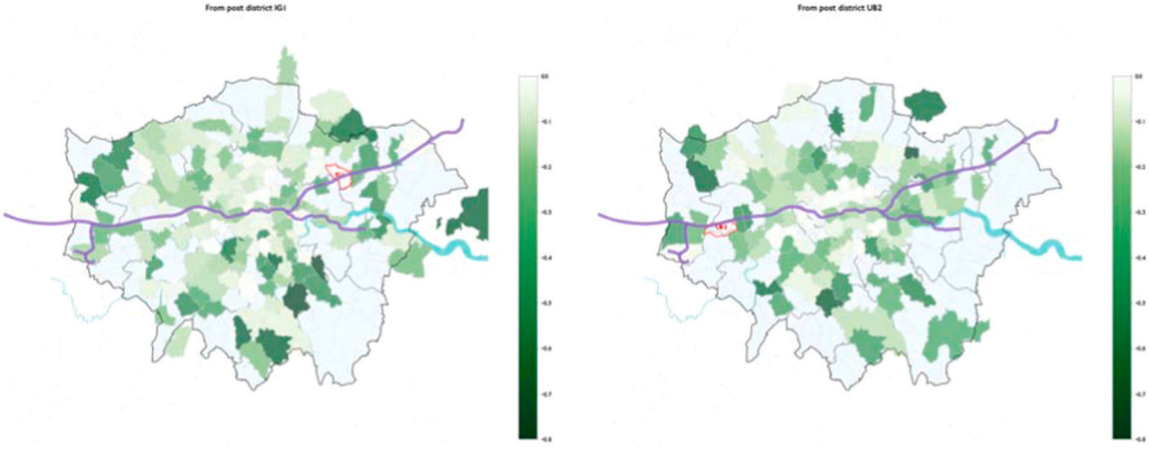

Fig. 4. Spatial distribution of GJT reduction for Case 4e_EZL (left) and 4w_EZL (right). All selected journeys with GJT reduction starting from Ilford (IG1: left) and Southall (UB2: right) are shown.

planning in London (Transport for London, 2017). This indicates that the service elasticity value found in our study is consistent with previous research.

5. Conclusions and recommendations

In this paper, we propose a smartcard based method to estimate the public transport service elasticity within an urban / metropolitan context. Based on more than 25 million empirical journeys subject to 9 different service interventions within the Greater London area, we find the average GJT elasticity to be −0.61. The value means that for every 1% increase in journey time, on average PT demand is expected to be reduced by 0.61%, and vice versa. We also find that the PT demand response to service changes is most elastic during the midday period between the peak hours, and most inelastic during the AM peak and early morning, possibly caused by a higher share of mandatory journeys. Our study results indicate that the elasticity figure increases with increasing time since the service change intervention, showing the existence of a build-up rate from the initial short-run elasticity to a somewhat stronger longer-run elasticity. Besides, we find that at least within the short- and medium-run demand is more elastic to service degradations compared to service improvements. An implication of this is that reversing previously implemented service reductions might not result in a full, symmetric PT demand recovery, and/or it will take longer before demand is fully recovered.

With our research we contribute to the development of a repeatable, direct methodology to estimate GJT elasticities for public transport planning based on empirical evidence resulting from individual passenger data and journey time data in a mode-agnostic manner. As discussed in Section 1.1, the resulting GJT elasticities are easier to use and simpler to understand than the existing appraisal methods relying on value of time and fare elasticity calculations. Our method can be used to quickly evaluate the relevant merit of different scheme options before investing resources into more complex simulation models or iterative business case refinements. This makes it potentially more receptive by business stakeholders in planning and appraisal processes. A key advantage of this research approach is the use of large volumes of disaggregated AFC data, in contrast to using indirect or aggregated rail ticket sales data as adopted in most journey time elasticity studies so far. Our method relies on generic AFC and AVL datasets as input that many transport operators have access to and frequently report on. This contributes to the transferability of our method, as different PT operators can easily adapt or apply the same approach to many case studies that naturally happen on their networks. The use of these automated datasets also means that value refresh can happen regularly, thereby maintaining recency and relevance.

The adoption of a mode-agnostic approach where the demand response is determined based on the full PT passenger journey made in the urban / metropolitan area of consideration has several implications. First, this approach better reflects the choice behaviour of passengers, who typically consider the impedance of the entire PT journey during mode choice or trip frequency choices. Second, it better aligns with the overarching PT perspective that PT authorities adopt, as our elasticities directly reflect the change in overall PT demand resulting from a service change. This provides a more direct insight in the change in PT mode share, which is often an important indicator for the extent of sustainable travel in an urban or a metropolitan area. Third, this perspective is consistent with the multimodal PT view adopted in most PT assignment models, where passenger route choice between origin and destination zones is generally not limited to a single PT mode. This implies that our found elasticity can be connected directly to modelled GJT changes resulting from PT assignments models. As the bus alighting stop of passengers is inferred, we should note that there is some degree of uncertainty regarding the final destination of a PT journey when the last leg is made by bus, despite the destination inference algorithm being validated extensively. Despite some uncertainty on the exact bus alighting stop, it is expected that in most cases the inferred alighting stop is located within the correct postcode district. As we aggregate demand and GJT to postcode districts in our study, the impact of this uncertainty on our study results is therefore expected to be small.

We formulate several recommendations for follow-up research. First, an area for further research is estimating GJT elasticities for weekends by extending the current input dataset. More generally, the estimation of GJT elasticities for different travel purposes or travel card types is recommended, as this is expected to drive the difference in elasticities found between different times of the day, and between different days of the week. Either by using passenger survey data or by inferring the most plausible journey purpose from AFC data, the estimation of purpose-specific elasticities could be explored. Second, it is recommended to study how a more detailed correction for background demand changes between pre-intervention baseline and post-intervention monitoring period can be included. This is relevant to better reflect the local background demand changes in an area affected by a service change by developing a more disaggregated procedure to correct for confounding effects. Third, so far service reliability has not been included in the GJT values used in this study. It is possible that the reliability by mode or route can sway passengers from trading a slower scheduled journey time for a more reliable journey. Incorporation of a reliability term in the GJT, such as the travel time variability or reliability buffer time, is recommended to capture this aspect explicitly within the GJT elasticity. At last, we recommend monitoring the demand response to service changes over a longer period of time. This can shine more light on the development of the elasticity figure after 1–3 years since the intervention. This can further contribute to understanding to what extent the asymmetric demand response found between service improvements and service degradations continues to exist in the long-run.

Declaration of Competing Interest

The authors declare that they have no known competing financial interests or personal relationships that could have appeared to influence the work reported in this paper.

References

Balcombe, R., Mackett, R., Paulley, N., Preston, J., Shires, J., Titheridge, H., Wardman, M., White, P., 2004. The Demand for Public Transport: A Practical Guide. TRL Report TRL593.

Bovy, P.H.L., Hoogendoorn-Lanser, S., 2005. Modelling route choice behaviour in multimodal transport networks. Transportation 32, 341–368.

Dargay, J.M., Hanly, M., 2002. The demand for local bus services in England. J. Transp. Econ. Policy 36, 73–91.

Eltved, M., Breyer, N., Ingvardson, J.B., Nielsen, O.A., 2021. Impact of long-term service disruptions on passenger travel behaviour: A smart card analysis from the Greater Copenhagen area. Transp. Res. Part C 131. https://doi.org/10.1016/j.trc.2021.103198.

Ferguson, E., 1992. Transit ridership, incident effects and public policy. Transp. Res. Part A 26, 393–407.

Gordon, J.B., 2012. Intermodal Passenger Flows on London's Public Transport Network. Automated Inference of Full Passenger Journeys Using Fare-transaction and Vehicle-location Data (M.Sc. thesis). Massachusetts Institute of Technology.

Gordon, J.B., Koutsopoulos, H.N., Wilson, N.H.M., Attanucci, J.P., 2013. Automated inference of linked transit journeys in London using fare-transaction and vehicle location data. Transp. Res. Rec. 2343, 17–24.

Jain, N., 2011. Assessing the Impact of Recent Fare Policy Changes on Public Transport Demand in London (M.Sc. thesis). Massachusetts Institute of Technology.

Kholodov, Y., Jenelius, E., Cats, O., Van Oort, N., Mouter, N., Cebecauer, M., Vermeulen, A., 2021. Public transport fare elasticities from smartcard data: Evidence from a natural experiment. Transp. Policy 105, 35–43.

Litman, T., 2019. Understanding Transport Demands and Elasticities. How Prices and Other Factors Affect Travel Behavior. Victoria Transport Policy Institute. http://www.vtpi.org/elasticities-.pdf.

Munizaga, M., Palma, C., 2012. Estimation of a disaggregate multimodal public transport origin-destination matrix from passive smart card data from Santiago, Chile. Transp. Res. Part C. 24, 9–18.

Neutens, T., Schwanen, T., Witlox, F., De Maeyer, P., 2010. Evaluating the temporal organisation of public service provision using space-time accessibility analysis. Urban Geogr. 31, 1039–1064.

Rail Delivery Group, 2018. Passenger Demand Forecasting Handbook v6.0. Passenger Demand Forecasting Council, UK.

Sánchez-Martinez, G.E., 2017. Inference of public transportation trip destinations by using fare transaction and vehicle location data: dynamic programming approach. Transp. Res. Rec. 2652, 1–7.
Shires, J.D., Ojeda-Cabral, M., Wardman, M., 2019. The impact of planned disruptions on rail passenger demand. Transportation 46, 1807–1837.
Transport for London, 2017. Business Case Development Manual. March 2017: V103.2017.03. ⟨https://foi.tfl.gov.uk/FOI-4306-1718/2017%20March%20BCDM%20S1701_Redacted.pdf⟩.
Transport for London, 2022. FOI Request Detail: Stations With/without Ticket Barriers on LU and LO. ⟨https://tfl.gov.uk/corporate/transparency/freedom-of-information/foi-request-detail?referenceId=FOI-0362-2223⟩.
Trépanier, M., Tranchant, N., Chapleau, R., 2007. Individual trip destination estimation in a transit smart card automated fare collection system. J. Intell. Transp. Syst. 11, 1–14.
Van Exel, N.J.A., Rietveld, P., 2001. Public transport strikes and traveller behaviour. Transp. Policy 8, 237–246.
Wang, Z.J., Li, X.H., Chen, F., 2015. Impact evaluation of a mass transit fare change on demand and revenue utilizing smart card data. Transp. Res. Part A 77, 213–224.
Wang, Z.J., Chen, F., Wang, B., Huang, J.-L., 2018. Passengers' response to transit fare change: an ex post appraisal using smart card data. Transportation 45, 1559–1578.
Wardman, M., 2004. Public transport values of time. Transp. Policy 11, 363–377.
Wardman, M., 2012. Review and meta-analysis of UK time elasticities of travel demand. Transportation 39, 465–490.
Wardman, M., 2022. Meta-analysis of British time-related demand elasticity evidence: An update. Transp. Res. Part A 157, 198–214.
Yap, M.D., Cats, O., 2022. Analysis and prediction of ridership impacts during planned public transport disruptions. J. Public Transp. 24 https://doi.org/10.1016/j.jpubtr.2022.100036.
Yap, M.D., Nijenstein, S., Van Oort, N., 2018. Improving predictions of public transport usage during disturbances based on smart card data. Transp. Policy 61, 84–95.
Yap, M.D., Cats, O., Van Arem, B., 2020. Crowding valuation in urban tram and bus transportation based on smart card data. Transp. A 16, 23–42.
Yap, M.D., Wong, H., Cats, O., 2023. Public Transport Crowding Valuation in a Post-pandemic Era (In preparation).
Zhu, S., Levinson, D.M., 2012. Disruptions to transportation networks: a review. In: Levinson, D.M., Liu, H.X., Bell, M. (Eds.), Network Reliability in Practice. Springer, New York City.